

A Novel Chemical Biology Approach for Mapping of Polymyxin Lipopeptide Antibody Binding Epitopes

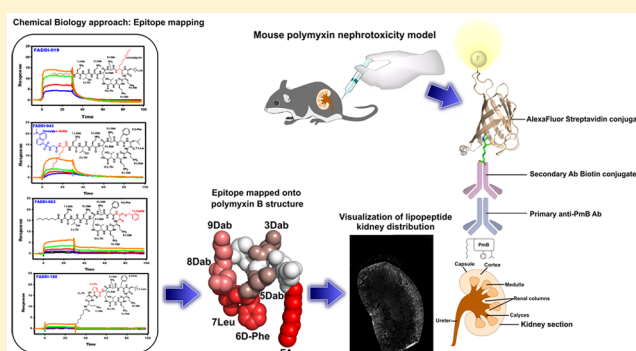
Tony Velkov,^{*,†} Bo Yun,^{†,‡} Elena K. Schneider,[†] Mohammad A. K. Azad,[†] Olan Dolezal,[§] Faye C. Morris,[†] Roger L. Nation,[†] Jiping Wang,[†] Ke Chen,[†] Heidi H. Yu,[†] Lv Wang,[†] Philip E. Thompson,[‡] Kade D. Roberts,^{†,‡} and Jian Li^{*,†}

[†]Drug Delivery, Disposition and Dynamics and [‡]Medicinal Chemistry, Monash Institute of Pharmaceutical Sciences, Monash University, Clayton, Victoria 3800, Australia

[§]CSIRO Manufacturing, Parkville, Victoria 3052, Australia

ABSTRACT: Polymyxins B and E (i.e., colistin) are a family of naturally occurring lipopeptide antibiotics that are our last line of defense against multidrug resistant (MDR) Gram-negative pathogens. Unfortunately, nephrotoxicity is a dose-limiting factor for polymyxins that limits their clinical utility. Our recent studies demonstrate that polymyxin-induced nephrotoxicity is a result of their extensive accumulation in renal tubular cells. The design and development of safer, novel polymyxin lipopeptides is hampered by our limited understanding of their complex structure–nephrotoxicity relationships. This is the first study to employ a novel targeted chemical biology approach to map the polymyxin recognition epitope of a commercially available polymyxin mAb and demonstrate its utility for mapping the kidney distribution of a novel, less nephrotoxic polymyxin lipopeptide. Eighteen novel polymyxin lipopeptide analogues were synthesized with modifications in the polymyxin core domains, namely, the N-terminal fatty acyl region, tripeptide linear segment, and cyclic heptapeptide. Surface plasmon resonance epitope mapping revealed that the monoclonal antibody (mAb) recognition epitope consisted of the hydrophobic domain (N-terminal fatty acyl and position 6/7) and diaminobutyric acid (Dab) residues at positions 3, 5, 8, and 9 of the polymyxin molecule. Structural diversity within the hydrophobic domains and Dab 3 position are tolerated. Enlightened with an understating of the structure–binding relationships between the polymyxin mAb and the core polymyxin scaffold, we can now rationally employ the mAb to probe the kidney distribution of novel polymyxin lipopeptides. This information will be vital in the design of novel, safer polymyxins through chemical tailoring of the core scaffold and exploration of the elusive/complex polymyxin structure–nephrotoxicity relationships.

KEYWORDS: *polymyxin, monoclonal antibody, epitope mapping, chemical biology*



Antibiotic resistance has evolved into a serious global health concern.^{1,2} In the United States, over 23,000 people die each year due to infections with antibiotic-resistant bacteria.^{3,4} Sadly, the “magic bullet” antibiotics we have used liberally over the past decades are rapidly losing their effectiveness. There has been a steady decline in the number of FDA-approved antibiotics, with only 10 antibiotics that are considered “new molecular entities” being approved by the FDA from 2004 to 2012.^{5,6} Medicine is clearly entering a critical period, and there could be catastrophic costs to healthcare and society if bacteria continue developing resistance to multiple antibiotics at the present rate and at the same time the pipeline continues to dry up.⁷ Modern healthcare over the past century has been founded on the basis that bacterial infections can be effectively treated using antibiotics. In a world without effective antibiotics, modern surgical and medical procedures that we take for granted will become too dangerous or impossible due to the threat of untreatable bacterial infections. This “perfect storm” has led to the revival of polymyxins B and E (colistin) as the

last-line therapy for infections caused by multidrug-resistant (MDR) Gram-negative pathogens.⁸

Polymyxins are cationic lipopeptides comprising hydrophobic and hydrophilic domains (amphipathicity), both of which are pivotal for their antibacterial activity. The core polymyxin scaffold consists of a cyclic heptapeptide linked to a linear tripeptide with an N-terminal fatty acyl tail (Figure 1). Five L- α,γ -diaminobutyric acid (Dab) residues decorate the scaffold, the primary amines of which are positively charged at physiological pH (7.4). Two hydrophobic residues in positions 6 and 7 of the cyclic heptapeptide form an intermediary hydrophobic segment that breaks the succession of cationic Dab residues. Polymyxin B and colistin are differentiated by a single hydrophobic residue at position 6: D-Phe in polymyxin B and D-Leu in colistin. Both polymyxins are secondary products

Received: February 19, 2016

Published: March 18, 2016

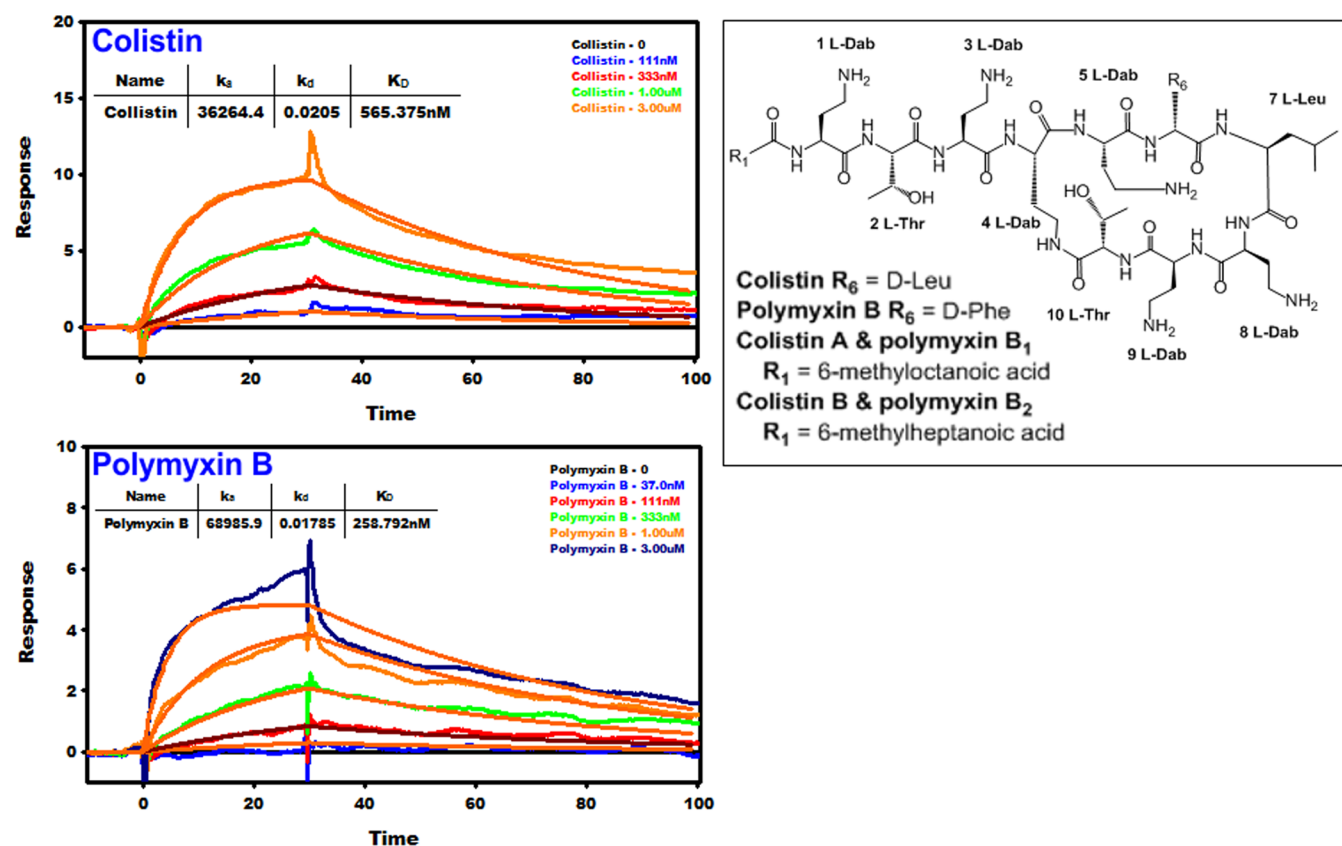


Figure 1. (Left panels) SPR sensograms for the binding of mAb clone 45 to colistin and polymyxin B. The inset shows the binding affinity values and the polymyxin concentration injected over the surface. (Right panel) Chemical structures of colistin and polymyxin B.

and are produced by fermentation as mixtures, containing two major components, colistins A and B and polymyxins B₁ and B₂, which differ by only by a single carbon at the N-terminal fatty acyl tail (i.e., C₇ vs C₈ fatty acyls) (Figure 1). Notwithstanding these differences, cross-resistance between colistin and polymyxin B exists.⁹

Despite their excellent antibacterial activity, the polymyxins have an Achilles' heel, namely, dose-limiting nephrotoxicity, which can occur in ~60% of patients.^{10–13} Polymyxin-induced nephrotoxicity is linked to their complex renal handling.^{14–16} Only a very small fraction of the dose is renally excreted.^{14–16} The polymyxins are filtered at the glomeruli and then undergo very extensive renal reabsorption, leading to accumulation in tubular cells.^{17–19} Our group has shown that, at concentrations achievable in patients considering the high risk of nephrotoxicity, resistance to the polymyxins can emerge rapidly in vitro in *Pseudomonas aeruginosa*, *Acinetobacter baumannii*, and *Klebsiella pneumoniae*,^{20–22} and resistance rates are increasing in isolates from patients.²³ Most worryingly, human infections caused by *Escherichia coli* that harbor plasmid-mediated colistin resistance have been recently reported in China and Switzerland, potentially as a result of the agricultural use of colistin in animal feed.^{24–26} Unfortunately, polymyxin resistance often implies a total lack of antibiotic treatment options for infections caused by MDR Gram-negative “superbugs”. Clearly, the development of a new generation of polymyxin lipopeptides with a wider therapeutic window is an urgent unmet global medical need.

Our research group is currently conducting a program to understand the mechanism of polymyxin-induced nephrotoxicity and discover new polymyxin lipopeptides with improved

efficacy and safety over the currently used polymyxin B and colistin. To this end we utilized a commercially available monoclonal antibody (mAb) raised to recognize polymyxin B to map the distribution of polymyxins in the kidneys. Immunohistochemical kidney disposition studies in animal models provide very valuable information on the kidney distribution of polymyxin B and colistin as well as our novel polymyxin lipopeptides. Because modifications to the polymyxin scaffold may have a significant influence on antibody recognition, it is important to understand the potential influence of structural differences on the structure-binding relationship with the polymyxin-mAb. Currently, the amino acid residues in the polymyxin B scaffold responsible for antibody binding are not known. Our objective was to undertake epitope mapping via surface plasmon resonance (SPR) screening of novel polymyxin lipopeptides from our extensive library that contains a diverse array of modifications to the core domains of the polymyxin scaffold. The ability to map the kidney distribution and structure–nephrotoxicity relationships (SNRs) of novel polymyxin lipopeptides will facilitate the chemical tailoring of their core scaffold to develop novel, safer polymyxins against MDR Gram-negative “superbugs”.

RESULTS AND DISCUSSION

Nephrotoxicity is the dose-limiting factor of the last-line antibiotics polymyxin B and colistin.^{27–29} We previously reported that polymyxin-induced nephrotoxicity results from the extensive accumulation of polymyxins in renal tubular cells with intracellular concentrations reaching 1930–4760-fold greater than the extracellular levels.¹⁷ The SNRs are a major

gap in the knowledge base for developing novel safer polymyxin-like lipopeptides. Toward this end, the present study employs a novel polymyxin lipopeptide library to perform SPR mapping of the polymyxin recognition epitope of a commercially available mAb and demonstrate its utility for mapping the kidney distribution of the novel polymyxin lipopeptide (FADDI-019) that we have previously shown to be less nephrotoxic than polymyxin B and colistin.^{30,31} The novel polymyxin lipopeptides screened for mAb binding contained a diverse array of structural modifications to the key structural domains of the polymyxin scaffold (Figure 1 and Table 1): (1) N-terminal fatty acyl group; (2) position 6/7 hydrophobic segment; and (3) hydrophilic (positively charged) Dab residues. The antimicrobial activity of the lipopeptides against a panel of polymyxin-susceptible and polymyxin-resistant clinical isolates of *P. aeruginosa*, *K. pneumoniae*,

A. baumannii, and *Enterobacter cloacae* are documented in Table 2 and discussed for each lipopeptide class below.

Role of the N-Terminal Fatty Acyl Group in Antibody Binding. The available SAR and SNR data suggest that the N-terminal fatty acyl domain of the polymyxins is essential for antibacterial activity and is partly responsible for the nephrotoxicity of polymyxins.^{32–40} Not surprisingly, most discovery programs have concentrated on generating semi-synthetic N-terminal analogues in an effort to discover safer polymyxins.^{36–38,41} The SPR epitope mapping data reveal that the mAb strongly recognized the octanoyl fatty acyl chain of the native polymyxin scaffold, as removal of the fatty acyl chain (colistin nonapeptide) abolished the binding. Replacement of the octanoyl fatty acyl chain (polymyxin B₁) with bulky hydrophobic substituents such as the 4-biphenylcarboxyl moiety (FADDI-020), dansylglycine-octylglycine (FADDI-043), dansylglycine (FADDI-053), or a 4-*tert*-butylphenylacetyl (FADDI-187) group decreased mAb binding affinity up to 22-fold for FADDI-053 (Figure 2 and Table 1). It is important to note that FADDI-020 also contained a modification to another structural domain, which had an influence on antibody binding, and likewise for FADDI-187 in which the Dab¹-Thr² segment was removed. It appears that whereas the N-terminal fatty acyl group was critical for antibody binding, the mAb was tolerant to some modification of this structural domain. In summary, the mAb preferentially recognized the linear C₈ fatty acyl chain, and bulky or aromatic substituents were poorly tolerated.

The MIC data revealed FADDI-020 displays an improved activity against the polymyxin-resistant strains of *P. aeruginosa*, *A. baumannii*, and *K. pneumoniae* (Table 2). The MICs of FADDI-020 against the polymyxin-susceptible strains were generally higher compared to those of polymyxin B and colistin.³¹ The MICs of FADDI-043 were fairly consistent, ranging from 4 to 16 mg/L across both the polymyxin-susceptible and -resistant strains examined.⁴² The MICs of FADDI-053 were largely comparable to those of polymyxin B and colistin, with an approximately 2-fold variation across most of the MICs. FADDI-187 was largely inactive against all of the test strains, showing activity (MICs = 1–2 mg/L) against only three of the polymyxin-susceptible strains tested.

Role of the Position 6/7 Hydrophobic Segment in Antibody Binding. In addition to the N-terminal fatty acyl chain, polymyxins feature a second hydrophobic domain, the position 6/7 segment in the heptapeptide ring that has been implicated in the plasma protein binding of polymyxins (Figure 1).⁴³ More importantly, we have previously reported that the substitution of the segment with D-octylglycine fatty acyl moieties significantly improved activity against polymyxin-resistant bacteria and lowered nephrotoxicity.³¹ The D-Phe⁶ acts as a turn-inducing residue that is critical for attaining the active β -turn conformation of the polymyxin molecule.^{44–46} The D-Phe⁶-L-Leu⁷ segment of polymyxin B appears to be important for mAb recognition. This is particularly evident with colistin, where a small reduction in the hydrophobicity within this segment as per the D-Leu⁶ substitution resulted in a 2-fold reduction in mAb binding affinity (Figures 1 and 2; Table 1). The hydrophobicity of the amino acids at this position was critical as evident from the substitution of either position 6 or 7 with methionine (FADDI-206 and FADDI-207), an amino acid structurally similar to leucine but less hydrophobic, which resulted in an up to 50-fold reduction in mAb binding affinity when compared to polymyxin B and colistin. Incorporation of a residue at position 6 (D-OctGly⁶ FADDI-019) or 7 (Cys(Bzl)⁷

Table 1. Monoclonal Antibody Binding Affinity Values for Polymyxin Lipopeptides

| polymyxin lipopeptide | polymyxin lipopeptide sequence ^a | K _D (μ M) |
|-----------------------|---|---------------------------|
| colistin | octanoyl-Dab-Thr-Dab-Dab*-Dab-D-Leu-Leu-Dab-Dab-Thr* | 0.56 |
| polymyxin B | octanoyl-Dab-Thr-Dab-Dab*-Dab-D-Phe-Leu-Dab-Dab-Thr* | 0.26 |
| FADDI-019 | octanoyl-Dab-Thr-Dab-Dab*-Dab-D-OctGly-Leu-Dab-Dab-Thr* | 0.43 |
| FADDI-020 | 4-biphenylcarboxyl-Dab-Thr-Dab-Dab*-Dab-D-OctGly-Leu-Dab-Dab-Thr* | 0.94 |
| FADDI-043 | dansylgly-OctGly-Dab-Thr-Dab-Dab*-Dab-D-Phe-Leu-Dab-Dab-Thr* | 2.71 |
| FADDI-063 | octanoyl-Dab-Thr-Dab-Dab*-Dab-D-Phe-Cys(Bz)-Dab-Dab-Thr* | 5.15 |
| FADDI-187 | 4- <i>tert</i> -butylphenylacetyl-D-Dab-Dab*-Dab-D-Phe-Leu-Dab-Dab-Thr* | 5.39 |
| FADDI-053 | dansylgly-Dab-Thr-Dab-Dab*-Dab-D-Phe-Leu-Dab-Dab-Thr* | 5.50 |
| FADDI-206 | octanoyl-Dab-Thr-Dab-Dab*-Dab-D-Phe-Met-Dab-Dab-Thr* | 8.80 |
| FADDI-065 | octanoyl-Dab-Thr-Lys-Dab*-Dab-D-Phe-Leu-Dab-Dab-Thr* | 13.1 |
| FADDI-207 | octanoyl-Dab-Thr-Dab-Dab*-Dab-D-Met-Leu-Dab-Dab-Thr* | 13.4 |
| FADDI-180 | octanoyl-Dab-Thr-Pro-Dab*-Dab-D-Phe-Leu-Dab-Dab-Thr* | 20.3 |
| FADDI-167 | octanoyl-Dab-Thr-Dab-Dab*-Dab-D-Phe-Leu-Ala-Dab-Thr* | NSB ^b |
| FADDI-168 | octanoyl-Dab-Thr-Dab-Dab*-Dab-D-Phe-Leu-Asn-Dab-Thr* | NSB |
| FADDI-169 | octanoyl-Dab-Thr-Dab-Dab*-Dab-D-Phe-Leu-Thr-Dab-Thr* | NSB |
| FADDI-170 | octanoyl-Dab-Thr-Dab-Dab*-Dab-D-Phe-Leu-Dab-Ala-Thr* | NSB |
| FADDI-171 | octanoyl-Dab-Thr-Dab-Dab*-Dab-D-Phe-Leu-Dab-Asn-Thr* | NSB |
| FADDI-172 | octanoyl-Dab-Thr-Dab-Dab*-Dab-D-Phe-Leu-Dab-Thr-Thr* | NSB |
| FADDI-175 | octanoyl-Dab-Thr-Dab-Dab*-Ala-D-Phe-Leu-Dab-Dab-Thr* | NSB |
| FADDI-176 | octanoyl-Dab-Thr-Dab-Dab*-Asn-D-Phe-Leu-Dab-Dab-Thr* | NSB |
| FADDI-177 | octanoyl-Dab-Thr-Dab-Dab*-Thr-D-Phe-Leu-Dab-Dab-Thr* | NSB |
| colistin nonapeptide | Thr-Dab-Dab*-Dab-D-Leu-Leu-Dab-Dab-Thr* | NSB |

^a* indicates the cyclization point. ^bNSB, no significant binding (K_D > 25 μ M).

Table 2. MICs (mg/L) of Polymyxin Lipopeptides against Gram-Negative Bacteria (Polymyxin-Resistant Isolates in Red)^a

| Polymyxin lipopeptide | Bacterial isolate | | | | | | | | | | | | | | | | | | | |
|-----------------------|---------------------------------|---------------------------------|----------------------------------|----------------------------------|----------------------------------|----------------------------------|--------------------------------|---------------------------------|--------------------------------|---------------------------------|---------------------------------|---------------------------------|---------------------------------|----------------------------------|----------------------------------|----------------------------------|----------------------------------|-------------------------------|-------------------------------|-------------------------------|
| | <i>P. aeruginosa</i> ATCC 27853 | <i>P. aeruginosa</i> FADDIPA001 | <i>P. aeruginosa</i> FADDI-PA025 | <i>P. aeruginosa</i> FADDI-PA070 | <i>P. aeruginosa</i> FADDI-PA060 | <i>P. aeruginosa</i> FADDI-PA090 | <i>A. baumannii</i> ATCC 19606 | <i>A. baumannii</i> FADDI-AB110 | <i>A. baumannii</i> ATCC 17978 | <i>A. baumannii</i> FADDI-AB065 | <i>A. baumannii</i> FADDI-AB156 | <i>A. baumannii</i> FADDI-AB167 | <i>K. pneumoniae</i> ATCC 13883 | <i>K. pneumoniae</i> FADDI-KP032 | <i>K. pneumoniae</i> FADDI-KP027 | <i>K. pneumoniae</i> FADDI-KP003 | <i>K. pneumoniae</i> FADDI-KP012 | <i>E. cloacae</i> FADDI-EC006 | <i>E. cloacae</i> FADDI-EC001 | <i>E. cloacae</i> FADDI-EC003 |
| Colistin | 1 | 1 | 2 | >128 | >128 | 8 | 1 | 0.5 | 0.5 | 128 | 16 | 8 | 1 | 1 | >128 | 128 | 32 | <0.125 | 0.25 | <0.125 |
| Polymyxin B | 1 | 1 | 1 | 32 | >32 | 4 | 1 | 0.5 | 1 | 128 | 8 | 16 | 1 | <0.125 | 128 | >32 | 16 | 0.5 | 0.25 | 0.5 |
| FADDI-019 | 4 | 4 | 8 | 4 | 2 | 8 | 1 | 4 | / | 32 | 16 | 8 | 4 | 4 | >32 | 32 | 16 | 2 | 1 | 1 |
| FADDI-020 | 2 | 4 | 4 | 2 | 2 | 8 | 4 | 2 | / | 32 | 4 | 4 | 4 | 2 | >32 | >32 | 8 | 4 | 4 | 2 |
| FADDI-043 | 4 | 4 | 4 | 4 | 4 | 4 | 4 | 8 | 4 | 4 | 8 | 4 | 8 | 16 | / | / | / | / | / | / |
| FADDI-053 | 2 | 2 | 2 | >32 | / | 16 | 4 | 2 | 1 | >32 | 32 | 8 | 2 | / | / | / | / | / | / | / |
| FADDI-063 | 1 | / | / | >32 | / | / | 1 | / | / | >32 | 2 | / | 16 | / | / | / | / | / | / | / |
| FADDI-065 | 2 | 2 | 8 | >32 | >32 | 32 | 2 | 1 | / | >32 | 32 | 32 | 0.25 | 0.5 | >32 | >32 | >32 | 1 | 0.5 | 0.5 |
| FADDI-167 | 2 | 2 | 32 | >32 | >32 | >32 | 16 | 16 | / | >32 | >32 | >32 | >32 | 1 | >32 | >32 | >32 | 8 | 1 | 2 |
| FADDI-168 | 2 | 4 | 14 | >32 | >32 | 4 | 4 | 8 | / | >32 | >32 | >32 | >32 | 0.5 | >32 | >32 | >32 | 0.5 | 0.5 | 0.5 |
| FADDI-169 | 2 | 4 | 16 | >32 | >32 | >32 | 16 | 32 | / | >32 | >32 | >32 | >32 | 1 | >32 | >32 | 8 | 8 | 1 | 2 |
| FADDI-170 | 2 | 4 | 32 | >32 | >32 | >32 | >32 | >32 | / | >32 | >32 | >32 | >32 | 4 | >32 | >32 | >32 | 8 | 8 | 8 |
| FADDI-171 | 2 | 4 | 8 | 8 | 8 | 8 | >32 | >32 | / | >32 | >32 | >32 | >32 | 8 | >32 | >32 | >32 | 8 | 16 | 8 |
| FADDI-172 | 4 | 4 | >32 | >32 | >32 | >32 | >32 | >32 | / | >32 | >32 | >32 | >32 | 4 | >32 | >32 | >32 | >32 | 8 | 16 |
| FADDI-175 | >32 | >32 | >32 | >32 | >32 | >32 | >32 | >32 | / | >32 | >32 | >32 | >32 | >32 | >32 | >32 | >32 | >32 | 32 | 32 |
| FADDI-176 | >32 | 16 | >32 | >32 | >32 | >32 | >32 | >32 | / | >32 | >32 | >32 | >32 | >32 | >32 | >32 | >32 | >32 | >32 | >32 |
| FADDI-177 | >32 | >32 | >32 | >32 | >32 | >32 | >32 | >32 | / | >32 | >32 | >32 | >32 | >32 | >32 | >32 | >32 | >32 | >32 | >32 |
| FADDI-180 | >32 | >32 | >32 | >32 | >32 | >32 | >32 | >32 | / | >32 | >32 | >32 | >32 | >32 | >32 | >32 | >32 | >32 | >32 | >32 |
| FADDI-187 | 1 | 2 | 2 | >32 | >32 | >32 | >32 | >32 | / | >32 | >32 | >32 | >32 | 4 | >32 | >32 | >32 | 16 | 26 | 8 |
| FADDI-206 | 1 | 1 | 4 | >32 | >32 | >32 | 1 | 1 | / | >32 | 8 | 2 | 2 | 0.25 | >32 | >32 | >32 | 0.5 | 0.25 | 0.25 |
| FADDI-207 | 1 | 2 | 4 | >32 | >32 | >32 | 8 | 8 | / | >32 | >32 | 16 | 16 | 0.25 | >32 | >32 | >32 | 1 | 0.25 | 0.5 |

^a/ = not determined.

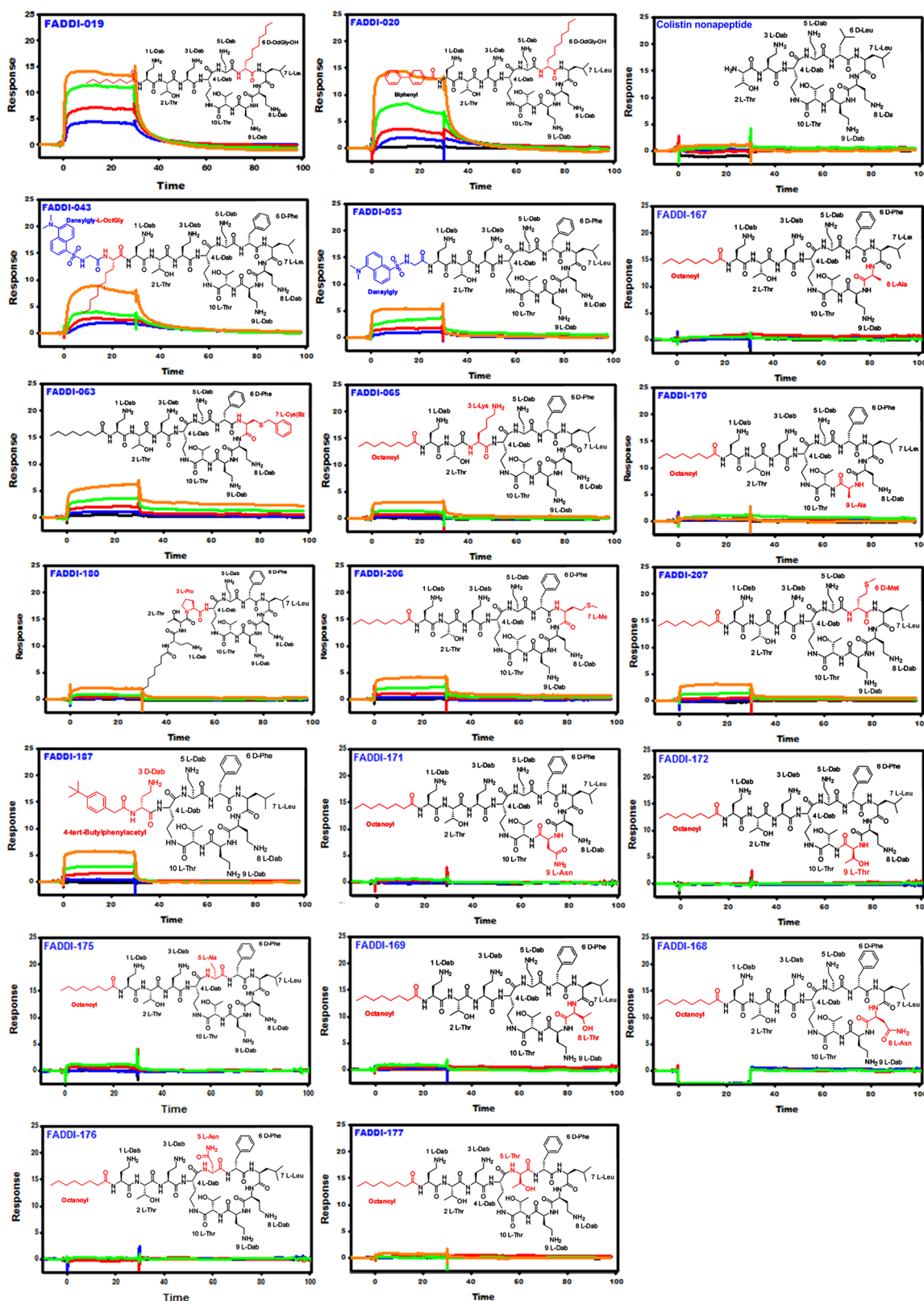


Figure 2. SPR sensograms for the binding of mAb clone 45 to novel polymyxin lipopeptides (black, 0.0 μM ; blue, 0.037 μM ; red, 0.11 μM ; green, 0.33 μM ; orange, 1.0 μM ; dark blue, 3.0 μM). The insets show the chemical structure of each lipopeptide, and the modified regions that differ from the polymyxin B core scaffold are colored red.

FADDI-063) with increased hydrophobicity resulted in \sim 2- and 19-fold reductions in mAb binding affinity, respectively. Together these results demonstrated that the hydrophobic position 6/7 segment is important for mAb recognition.

In terms of the antibacterial activity, the hydrophobic side chains of the position 6/7 segment are believed to insert into the bacterial outer membrane (OM) and help stabilize complex formation with LPS through hydrophobic interactions with the

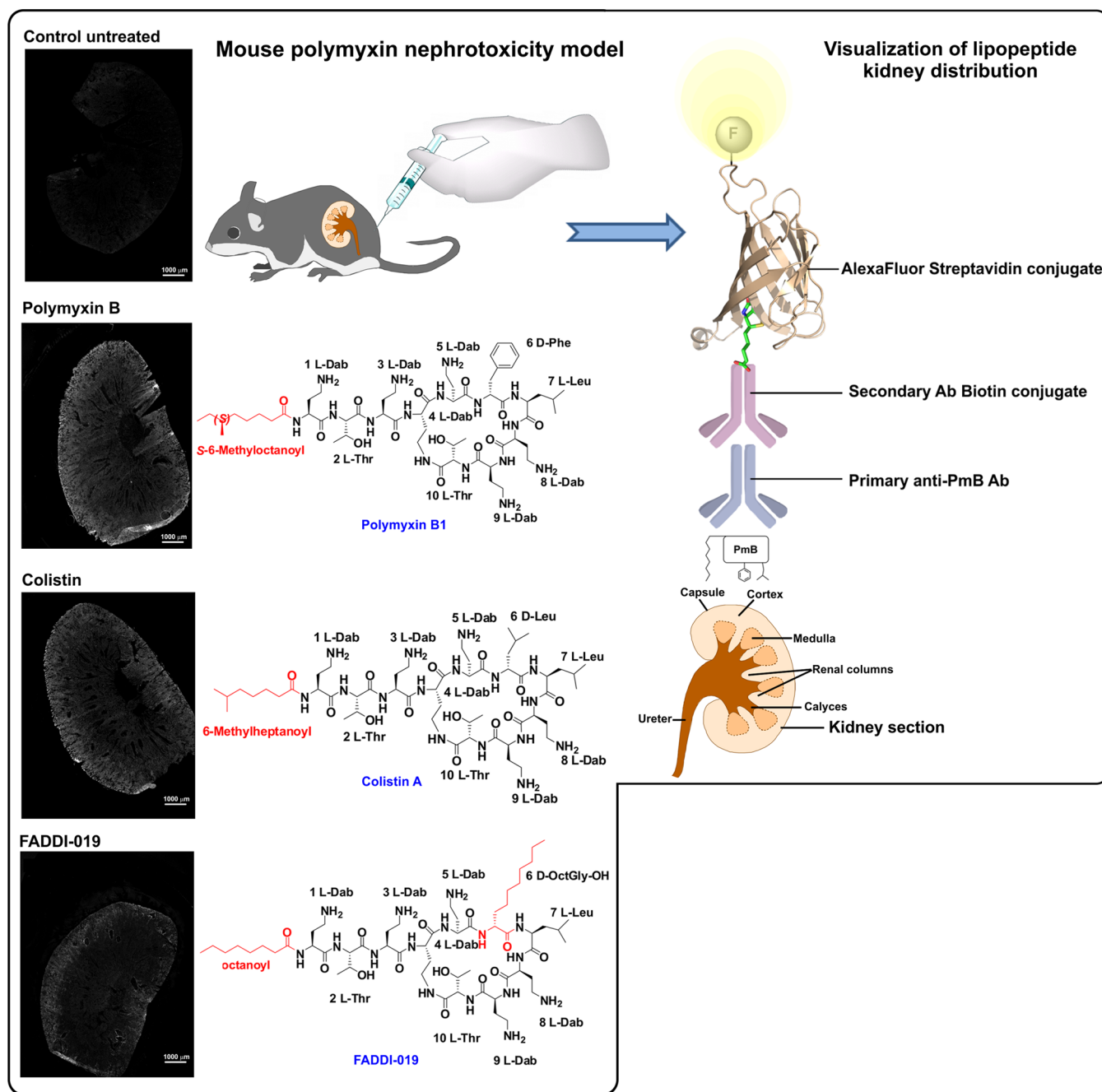


Figure 3. Immunohistochemical staining with mAb clone 45 of kidney sections from mice treated with polymyxin lipopeptides. (Right side) Schematic diagram of the mouse nephrotoxicity model and in situ image development procedure employed for the visualization of the kidney distribution of the polymyxin lipopeptides.

lipid A fatty acyl chains.^{45,46} The MIC data revealed that FADDI-019 is similarly antibacterial as FADDI-020 with an improved activity against the polymyxin-resistant strains of *P. aeruginosa*, *A. baumannii*, and *K. pneumoniae* (Table 2).³¹ The MICs of FADDI-019 were generally lower against the polymyxin-susceptible strains compared to polymyxin B and colistin. FADDI-206 and FADDI-207 showed MICs generally comparable to those of polymyxin B and colistin.

Role of the Hydrophilic Positively Charged Dab Residues in Antibody Binding. In addition to the two aforementioned hydrophobic regions, the positive charges of the five Dab residues were also identified as major nephrotoxic “hot spots” in the polymyxin scaffold.^{8,19,39,47–52} The epitope

mapping data revealed that the Dab residues at positions 5 (FADDI 175–177), 8 (FADDI 167–169), and 9 (FADDI 170–172) are critical for mAb recognition as substitution at any of these positions led to a complete loss of mAb binding (Figures 1 and 2; Table 1). The mAb also appeared to recognize the Dab³ position as the exchange of Dab³ with a lysine residue (FADDI-065) resulted in a 44-fold decrease in binding affinity, whereas a change to a Pro (FADDI-180) resulted in a 67-fold decrease in binding affinity. In summary, the mAb preferentially recognized the cationic Dab residues at positions 3, 5, 8, and 9 of the polymyxin molecule.

The exact order of the Dab residues within the primary sequence of the polymyxin scaffold ensures the correct

placement of the positive charges for electrostatic interactions with the negative phosphates of lipid A, which is critical for antimicrobial activity.⁵¹ The MIC data revealed FADDI-175, FADDI-176, FADDI-177, and FADDI-180 were inactive against all of the strains tested with MICs > 32 mg/L. The MIC profiles of the lipopeptides FADDI-065, FADDI-167, FADDI-168, FADDI-169, FADDI-170, FADDI-171, and FADDI-172 were very similar; all of these lipopeptides were largely inactive, except against a few of the polymyxin-susceptible strains of *P. aeruginosa* (MICs 2–8 mg/L) and *K. pneumoniae* FADDI-KP032 (MICs 0.5–8 mg/L) and against the three *E. cloacae* strains tested (MICs 0.5–16 mg/L).

Imaging the Localization of Polymyxins in Bacterial Cells and Mouse Kidneys Using the Polymyxin B mAb.

As a proof-of-concept, we employed in situ immunohistochemical staining of the kidney sections from a mouse treated with polymyxin B (D-Phe⁶-L-Leu⁷), colistin (D-Leu⁶-L-Leu⁷), and the novel FADDI-019 (D-octylglycine⁶-L-Leu⁷), which we have previously shown to be less nephrotoxic than polymyxin B and colistin.³¹ The imaging data revealed that polymyxin B and colistin were predominantly distributed within the renal cortex and to a lesser extent within the medulla of the kidney (Figure 3). These findings are in line with our recent immunohistochemical and correlative microscopy studies, which demonstrated that polymyxins accumulate at extremely high concentrations within renal tubular cells of the renal cortex.^{17,19}

In contrast, FADDI-019, in which position 6 is substituted with a more hydrophobic D-octylglycine amino acid, was distributed largely within the outer layer of the renal cortex. Our recent data demonstrate that increasing the hydrophobicity of position 7 can substantially increase plasma protein binding of polymyxin molecules.³¹ Differences in pharmacokinetics may cause the different localization of polymyxins in the mouse kidney as shown using the polymyxin B mAb, and further pharmacological studies are warranted (Figure 3).

Polymyxins exert their antimicrobial activity through an electrostatic interaction of the cationic Dab residues with the negatively charged phosphate groups of lipid A of LPS. This complex formation displaces divalent cations (Ca²⁺ and Mg²⁺) that bridge adjacent LPS molecules.^{8,51,53} Subsequently, hydrophobic interactions occur between the N-terminal fatty acyl tail and the position 6 and 7 hydrophobic segment of the polymyxin molecule and the lipid A fatty acyl chains, thereby becoming imbedded in the bacterial OM. It is hypothesized that this “self-promoted” uptake mechanism leads to disruption of the cell envelope, resulting in bacterial killing.^{51,54–56} To further validate the epitope mapping data, we attempted to employ the mAb to detect polymyxin B on *A. baumannii* ATCC19606 cells. Interestingly, the mAb was unable to detect polymyxin B in the OM of *A. baumannii* cells (data not shown). Presumably, once the polymyxin B has complexed with lipid A,⁵¹ its hydrophobic domains (that form most of the mAb recognition epitope) become imbedded in the OM and are therefore shielded from mAb binding.

CONCLUSIONS

In summary, this is the first chemical biology study to map the polymyxin recognition epitope of a commercially available polymyxin mAb. Both the hydrophobic domains (N-terminal fatty acyl and position 6/7) and Dab residues, in particular, Dabs 3, 5, 8, and 9, of the polymyxin are components of the polymyxin mAb recognition epitope (Figure 4). Notwithstanding, the lipopeptide library SPR screening and FADDI-019

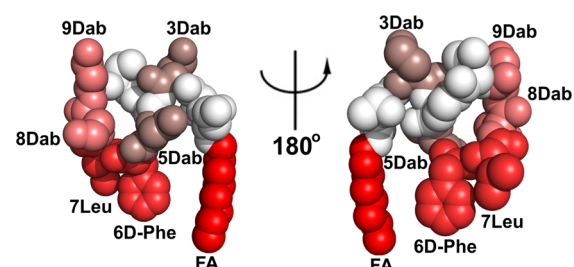


Figure 4. Monoclonal antibody clone 45 epitope “hot spots” on the polymyxin B structure. The SPR K_D values were mapped onto the NMR solution structure of polymyxin B₁ (higher affinity binding is represented by a brighter red coloring). The polymyxin B₁ structure is shown in CPK representation, and the two views are rotated by 180° about the y-axis.

imaging data indicate that structural diversity within the hydrophobic domains and Dab 3 position are tolerated. This means that the mAb may be of considerable utility for probing the kidney distribution of novel polymyxin lipopeptides, as we have demonstrated using FADDI-019. The ability to effectively map the kidney distribution of novel polymyxin lipopeptides using a polymyxin-specific mAb with a defined epitope map will facilitate the elucidation of the ever-elusive structure–nephrotoxicity relationships of the polymyxins. This in turn may open up opportunities for the development of novel, safer polymyxins through the careful chemical tailoring of the core scaffold.

EXPERIMENTAL PROCEDURES

Chemical Reagents. Anti-polymyxin B mouse IgM antibody (clone 45) was obtained from Thermo Fisher Scientific (Rockford, IL, USA). Polymyxin B (sulfate), colistin (sulfate), triisopropylsilane (TIPS), trifluoroacetic acid (TFA), diphenylphosphorylazide (DPPA), and streptavidin were purchased from Sigma-Aldrich (Sydney, NSW, Australia). Piperidine and diisopropylethylamine (DIPEA) were obtained from Auspep (Melbourne, VIC, Australia). Fmoc-Dab(Boc)-OH was purchased from Try-lead Chem (Hangzhou, Zhejiang, China). Fmoc-Thr(tBu)-OH and Fmoc-Leu-OH were from Mimotopes (Melbourne, Australia). Fmoc-Dab(ivDde)-OH, Fmoc-D-Phe-OH, and 1*H*-benzotriazolium-1-[bis(dimethylamino)methylene]-5-chlorohexafluoro-phosphate-(1-),3-oxide (HCTU) were purchased from Chem-Impex International (Wood Dale, IL, USA). Fmoc-Thr(tBu)-TCP-resin was obtained from Intavis Bioanalytical Instruments (Köln, Germany). Dimethylformamide (DMF), methanol (MeOH), diethyl ether, dichloromethane (DCM), and acetonitrile were purchased from Merck (Melbourne, VIC, Australia). Polymyxin lipopeptide stock solutions were prepared with Milli-Q water (Millipore, North Ryde, NSW, Australia) and filtered using 0.22 μm syringe filters (Sartorius, Melbourne, VIC, Australia). Solutions were stored at 4 °C for up to 1 month.⁵⁷

Lipopeptide Synthesis. Synthesis procedures for specific lipopeptides were previously described in detail by our group.^{31,58} Briefly, the protected linear peptides were synthesized on a CEM Liberty Microwave automated peptide synthesizer using Fmoc solid-phase peptide chemistry. Synthesis was carried out using TCP-resin, preloaded with Fmoc-Thr(tBu)-OH was carried out using TCP-resin, preloaded with Fmoc-Thr(tBu)-OH (0.1 mmol scale). Fmoc-amino acid coupling and the N-terminal group were performed as follows: 5 mol equiv of Fmoc amino acid and HCTU with activation

using DIPEA in DMF over 2 min at room temperature and then for 4 min at 50 °C (25 W microwave power). Fmoc deprotection was performed as follows: 20% piperidine in dimethylformamide (1 × 30 s, 1 × 3 min) at 75 °C (35 W microwave power). Resin was removed from the synthesizer, transferred to a synthesis syringe, and treated with 2% hydrazine in DMF (4 × 15 min), removing the ivDde group. The resin was then washed with MeOH (2 × 2 min) and diethyl ether (1 × 2 min) and air-dried under vacuum. The protected linear peptide was cleaved from the resin by washing with 1% TFA in DCM (1 × 5 min, 3 × 10 min). The residue was dissolved in 50% acetonitrile/water and freeze-dried. The protected linear peptide was dissolved in DMF (10 mL) to which DPPA (3 equiv relative to the loading of the resin) and DIPEA (6 equiv relative to the loading of the resin) were added. The solution was stirred overnight at room temperature and then concentrated under vacuum. The residue was taken up in a solution of 5% TIPS in TFA and stirred at room temperature for 2 h. TFA was removed under a nitrogen stream, and the crude cyclic peptide was precipitated with cold diethyl ether, collected by centrifugation, and air-dried. The residue was then taken up in Milli-Q water and desalted with a Vari-Pure IPE SAX column. The crude cyclic lipopeptide was subjected to RP-HPLC purification and LC-MS analysis as described below.

HPLC Purification and LC-MS Analysis of Lipopeptides. Crude cyclic lipopeptides were purified by RP-HPLC on a Waters Prep LC system with a Waters 486 tunable absorbance detector (214 nm). A Phenomenex Axia column (Luna C8(2), 250 × 21.2 mm i.d., 100 Å, 10 μm) was employed with a gradient of 0–60% buffer B over 60 min at a flow rate of 15 mL/min; buffer A was 0.1% TFA/water, and buffer B was 0.1% TFA/acetonitrile. Collected fractions were analyzed using a Shimadzu 2020 LCMS system, with a photodiode array detector (214 nm) coupled to an electrospray ionization source and a single-quadrupole mass analyzer. RP-HPLC was performed with a Phenomenex column (Luna C8(2), 100 × 2.0 mm i.d.) with an eluting gradient of 80% acetonitrile in 0.05% aqueous TFA over 10 min at 0.2 mL/min (buffer A, 0.05% TFA/water; buffer B, 0.05% TFA/acetonitrile). Mass spectra were acquired in the positive ion mode in the scan range of m/z 200–2000.

Bacterial Strains and MIC Determination. *P. aeruginosa*, *K. pneumoniae*, *A. baumannii*, and *E. cloacae* strains were obtained from the American Type Culture Collection (Rockville, Maryland, USA) or were clinical isolates. Bacterial isolates were stored at –80 °C in tryptone soy broth (Oxoid, Thermo Fisher Scientific, Adelaide, South Australia, Australia) with 20% glycerol (Ajax Finechem, Seven Hills, New South Wales, Australia). The MICs of the polymyxin lipopeptides were determined by broth microdilution.⁵⁹ Experiments were performed with Cation-adjusted Mueller-Hinton Broth (CaMHB) in 96-well polypropylene microtiter plates. Wells were inoculated with 100 μL of bacterial suspension prepared in CaMHB (containing ~10⁶ colony forming units (cfu) per mL) and 100 μL of CaMHB containing increasing concentrations of the lipopeptide (0 to 128 mg/L). The MIC was defined as the lowest concentration at which visible growth was inhibited following 18 h incubation at 37 °C.

Surface Plasmon Resonance. Immobilization of the anti-polymyxin B mouse IgM monoclonal antibody onto a CMS sensor chip surface was achieved using a double-capture method that utilized a streptavidin-coated chip to load biotin

anti-IgM conjugate (CaptureSelect, Life Technologies, Melbourne, VIC, Australia) followed by a capture of the IgM antibody. Streptavidin was simultaneously immobilized in all four channels of a CMS sensor chip docked in a Biacore T200 instrument equilibrated with 1× HBS-P+ buffer (10 mM HEPES, pH 7.4, 150 mM NaCl, 0.05% (v/v) Tween-20). Immobilization was performed at 37 °C at a constant flow rate of 10 μL/min, using standard amide coupling chemistry recommended by the chip manufacturer. Streptavidin was diluted in 10 mM sodium acetate buffer, pH 4.5, to a final concentration of 100 μg/mL. This approach resulted in immobilization of 12500 response units (1 RU = 1 pg protein/mm²) with minimal variation between the four channels on the same chip. Freshly immobilized streptavidin surfaces were further conditioned with three consecutive 30 s injections of conditioning solution consisting of 50 mM NaOH and 1 M NaCl. All subsequent capture and binding experiments were performed at 25 °C with 1× HBS-EP+ as instrument running buffer (10 mM HEPES, pH 7.4, 150 mM NaCl, 3 mM EDTA, 0.05% (v/v) Tween-20). CaptureSelect biotin anti-IgM conjugate was diluted to 10 μg/mL in 1× HBS-EP+ and injected onto a streptavidin chip surface in channels 3 and 4 at 10 μL/min for 420 s, resulting in a capture of approximately 7500 RU of protein. Anti-polymyxin B mouse IgM was diluted 1:100 in 1× HBS-EP+ and injected in channel 4 only at 5 μL/min two times for 120 s each. After allowing the captured anti-polymyxin B mouse IgM baseline to stabilize for 3 min, final captured levels were estimated to be ~1450 RU. To evaluate binding interactions, serial dilutions of polymyxin lipopeptides (cf. Table 1) were prepared in 1× HBS-EP+ buffer and sequentially injected over immobilized proteins in channels 3 and 4 with the association and dissociation phases monitored for 30 and 180 s, respectively. Control injections of the instrument running buffer (“zero-buffer” blank solution) were also included for double-referencing purposes. No regeneration of anti-polymyxin B mouse IgM surface was required between binding cycles as bound polymyxin lipopeptides fully dissociated within 60–180 s in the running buffer. All SPR sensorgrams were processed using Scrubber software (www.biologic.com.au). Sensorgrams were first zeroed on the y-axis and then x-aligned at the beginning of each injection. Bulk refractive index changes were removed by subtracting the response of the reference flow cell (channel 3) responses. The average response of all blank injections was subtracted from all analyte injections and blank sensorgrams to remove systematic artifacts in the experimental and reference flow cells. Scrubber software was then used to extract k_a and k_d rate parameters from the processed data sets by globally fitting to a 1:1 binding model. The affinity (K_D) was calculated from the quotient k_d/k_a . Alternatively, for rapidly dissociating interactions, K_D estimates were derived using steady-state affinity algorithm.

Epitope Mapping onto the Polymyxin B Structure. The Ab binding epitope was mapped onto the three-dimensional structure of polymyxin B using the coordinates from the NMR solution structure of polymyxin B₁ when bound to *E. coli* LPS.^{45,46} Molecular visualization was performed using the software package PYMOL (Schrödinger, Cambridge, MA, USA).

Immunostaining of Polymyxins in Mouse Kidneys and Bacterial Cells. The animal study was approved by the Monash Institute of Pharmaceutical Sciences Animal Ethics Committee and performed in accordance with the Australian National Health and Medical Research Council (NHMRC)

guidelines for the care and use of animals for scientific purposes. Female Swiss mice (6–8 weeks old, 20–25 g) had free access to food and water during the experiment. Polymyxin B, colistin, FADDI-019, or sterile saline was administered subcutaneously to mice ($n = 3$) over 3 days (accumulated dose of 175 mg/kg, with 35, 10, 10, or 20 mg/kg administered at 2 h intervals on day 1; 35, 10, 10, or 15 mg/kg at 2 h intervals on day 2; and a final dose of 30 mg/kg on day 3). Mice were euthanized on day 3 via isoflurane overdose 2 h after the last dose, and kidneys were collected, frozen, and sectioned at 12 μm . Sections were fixed in cold acetone, dried, and treated with 1% hydrogen peroxide (5 min). Endogenous mouse IgG was blocked using the Vector M.O.M kit (Vector Laboratories, Burlingame, CA, USA) as per the manufacturer's instructions. Sections were incubated with anti-polymyxin B mouse IgM mAb diluted to 1:500 overnight at 4 °C, washed, and incubated with M.O.M biotinylated anti-mouse secondary link (Vector Laboratories) for 10 min. Following incubation with Alexa-Fluor647 streptavidin conjugate (1:500) (Life Technologies, Melbourne, VIC, Australia), sections were mounted with Dako fluorescence mounting medium (Dako, Sydney, NSW, Australia) and imaged using a MetasystemsVSlide Scanner.

For detection of polymyxin B bound to bacterial cells, exponential phase *A. baumannii* ATCC19606 cells (OD 600 nm 0.1) were harvested by centrifugation and washed twice with PBS. The cells were then treated with polymyxin B at $\times 0.5$ MIC (0.5 mg/L) for 1 h and washed with PBS. The cells were then incubated for 5 h with anti-polymyxin B mouse IgM mAb diluted to 1:500 at 4 °C, washed twice with PBS, and imaged as described above.

AUTHOR INFORMATION

Corresponding Authors

*(J.L.) Phone: +61 3 9903 9702. Fax: +61 3 9903 9583. E-mail: colistin.polymyxin@gmail.com.

*(T.V.) E-mail: Tony.Velkov@monash.edu

Notes

The authors declare no competing financial interest.

ACKNOWLEDGMENTS

J.L., T.V., R.L.N., P.E.T., and K.D.R. are supported by a research grant from the National Institute of Allergy and Infectious Diseases of the National Institutes of Health (R01 AI098771), and J.L. and T.V. are also supported by R01 AI111965. The content is solely the responsibility of the authors and does not necessarily represent the official views of the National Institute of Allergy and Infectious Diseases or the National Institutes of Health. J.L. is an Australian NHMRC Senior Research Fellow. T.V. is an Australian NHMRC Industry Career Development Research Fellow.

ABBREVIATIONS

Bz, benzyl; CaMHB, cation-adjusted Mueller–Hinton broth; Dab, diaminobutyric acid; K_D , binding affinity constant; LPS, lipopolysaccharide; MeOH, methanol; MIC, minimum inhibitory concentration; MDR, multidrug resistant; OM, outer membrane; SNR, structure–nephrotoxicity relationships; TFA, trifluoroacetic acid

REFERENCES

(1) Wernli, D., Hausteiner, T., Conly, J., Carmeli, Y., Kickbusch, I., and Harbarth, S. (2011) A Call for Action: The Application of the

International Health Regulations to the Global Threat of Antimicrobial Resistance. *PLoS Med.* 8 (4), e1001022.

(2) Lodato, E. M., Kaplan, W. (2013) *Background Paper 6.1 Antimicrobial Resistance*, World Health Organization.

(3) Ventola, C. L. (2015) The antibiotic resistance crisis: part 2: management strategies and new agents. *P&T Community* 40 (5), 344–352.

(4) Ventola, C. L. (2015) The antibiotic resistance crisis: part 1: causes and threats. *P&T Community* 40 (4), 277–283.

(5) The bacterial challenge: time to react. *EJHP Practice* 2009, 15 (5), 15.10.2900/2518

(6) Boucher, H. W., Talbot, G. H., Bradley, J. S., Edwards, J. E., Gilbert, D., Rice, L. B., Scheld, M., Spellberg, B., and Bartlett, J. (2009) Bad bugs, no drugs: no ESKAPE! An update from the Infectious Diseases Society of America. *Clin. Infect. Dis.* 48 (1), 1–12.

(7) Cars, O., Hogberg, L. D., Murray, M., Nordberg, O., Sivaraman, S., Lundborg, C. S., So, A. D., and Tomson, G. (2008) Meeting the challenge of antibiotic resistance. *BMJ.* 337, a1438.

(8) Velkov, T., Roberts, K. D., Nation, R. L., Thompson, P. E., and Li, J. (2013) Pharmacology of polymyxins: new insights into an 'old' class of antibiotics. *Future Microbiol.* 8 (6), 711–724.

(9) Li, J., Nation, R. L., Turnidge, J. D., Milne, R. W., Coulthard, K., Rayner, C. R., and Paterson, D. L. (2006) Colistin: the re-emerging antibiotic for multidrug-resistant Gram-negative bacterial infections. *Lancet Infect. Dis.* 6 (9), 589–601.

(10) Landman, D., Georgescu, C., Martin, D. A., and Quale, J. (2008) Polymyxins revisited. *Clin. Microbiol. Rev.* 21 (3), 449–465.

(11) Akajagbor, D. S., Wilson, S. L., Shere-Wolfe, K. D., Dakum, P., Charurat, M. E., and Gilliam, B. L. (2013) Higher incidence of acute kidney injury with intravenous colistimethate sodium compared with polymyxin B in critically ill patients at a tertiary care medical center. *Clin. Infect. Dis.* 57, 1300–1303.

(12) Hartzell, J. D., Neff, R., Ake, J., Howard, R., Olson, S., Paolino, K., Vishnepolsky, M., Weintrob, A., and Wortmann, G. (2009) Nephrotoxicity associated with intravenous colistin (colistimethate sodium) treatment at a tertiary care medical center. *Clin. Infect. Dis.* 48, 1724–1728.

(13) Kubin, C. J., Ellman, T. M., Phadke, V., Haynes, L. J., Calfee, D. P., and Yin, M. T. (2012) Incidence and predictors of acute kidney injury associated with intravenous polymyxin B therapy. *J. Infect.* 65 (1), 80–87.

(14) Li, J., Coulthard, K., Milne, R., Nation, R. L., Conway, S., Peckham, D., Etherington, C., and Turnidge, J. (2003) Steady-state pharmacokinetics of intravenous colistin methanesulphonate in patients with cystic fibrosis. *J. Antimicrob. Chemother.* 52 (6), 987–992.

(15) Li, J., Milne, R. W., Nation, R. L., Turnidge, J. D., Smeaton, T. C., and Coulthard, K. (2004) Pharmacokinetics of colistin methanesulphonate and colistin in rats following an intravenous dose of colistin methanesulphonate. *J. Antimicrob. Chemother.* 53 (5), 837–840.

(16) Sandri, A. M., Landersdorfer, C. B., Jacob, J., Boniatti, M. M., Dalarosa, M. G., Falci, D. R., Behle, T. F., Bordinhao, R. C., Wang, J., Forrest, A., Nation, R. L., Li, J., and Zavascki, A. P. (2013) Population pharmacokinetics of intravenous polymyxin B in critically ill patients: implications for selection of dosage regimens. *Clin. Infect. Dis.* 57, 524–531.

(17) Azad, M. A., Roberts, K. D., Yu, H. H., Liu, B., Schofield, A. V., James, S. A., Howard, D. L., Nation, R. L., Rogers, K., de Jonge, M. D., Thompson, P. E., Fu, J., Velkov, T., and Li, J. (2015) Significant accumulation of polymyxin in single renal tubular cells: a medicinal chemistry and triple correlative microscopy approach. *Anal. Chem.* 87 (3), 1590–1595.

(18) Yun, B., Azad, M. A., Nowell, C. J., Nation, R. L., Thompson, P. E., Roberts, K. D., Velkov, T., and Li, J. (2015) Cellular uptake and localization of polymyxins in renal tubular cells using rationally designed fluorescent probes. *Antimicrob. Agents Chemother.* 59 (12), 7489–7496.

- (19) Yun, B., Azad, M. A., Wang, J., Nation, R. L., Thompson, P. E., Roberts, K. D., Velkov, T., and Li, J. (2015) Imaging the distribution of polymyxins in the kidney. *J. Antimicrob. Chemother.* 70 (8), 827–829.
- (20) Poudyal, A., Howden, B. P., Bell, J. M., Gao, W., Owen, R. J., Turnidge, J. D., Nation, R. L., and Li, J. (2008) In vitro pharmacodynamics of colistin against multidrug-resistant *Klebsiella pneumoniae*. *J. Antimicrob. Chemother.* 62 (6), 1311–1318.
- (21) Bergen, P. J., Tsuji, B. T., Bulitta, J. B., Forrest, A., Jacob, J., Sidjabat, H. E., Paterson, D. L., Nation, R. L., and Li, J. (2011) Synergistic killing of multidrug-resistant *Pseudomonas aeruginosa* at multiple inocula by colistin combined with doripenem in an in vitro pharmacokinetic/pharmacodynamic model. *Antimicrob. Agents Chemother.* 55 (12), 5685–5695.
- (22) Deris, Z. Z., Yu, H. H., Davis, K., Soon, R. L., Jacob, J., Ku, C. K., Poudyal, A., Bergen, P. J., Tsuji, B. T., Bulitta, J. B., Forrest, A., Paterson, D. L., Velkov, T., Li, J., and Nation, R. L. (2012) The combination of colistin and doripenem is synergistic against *Klebsiella pneumoniae* at multiple inocula and suppresses colistin resistance in an in vitro pharmacokinetic/pharmacodynamic model. *Antimicrob. Agents Chemother.* 56 (10), 5103–5112.
- (23) Cai, Y., Chai, D., Wang, R., Liang, B., and Bai, N. (2012) Colistin resistance of *Acinetobacter baumannii*: clinical reports, mechanisms and antimicrobial strategies. *J. Antimicrob. Chemother.* 67 (7), 1607–1615.
- (24) Liu, Y.-Y., Wang, Y., Walsh, T. R., Yi, L.-X., Zhang, R., Spencer, J., Doi, Y., Tian, G., Dong, B., Huang, X., Yu, L.-F., Gu, D., Ren, H., Chen, X., Lv, L., He, D., Zhou, H., Liang, Z., Liu, J.-H., and Shen, J. (2016) Emergence of plasmid-mediated colistin resistance mechanism MCR-1 in animals and human beings in China: a microbiological and molecular biological study. *Lancet Infect. Dis.* 16 (2), 161–168.
- (25) Paterson, D. L., and Harris, P. N. A. (2016) Colistin resistance: a major breach in our last line of defence. *Lancet Infect. Dis.* 16, 132–133.
- (26) Poirel, L., Kieffer, N., Liassine, N., Thanh, D., and Nordmann, P. (2016) Plasmid-mediated carbapenem and colistin resistance in a clinical isolate of *Escherichia coli*. *Lancet Infect. Dis.* 16, 281.
- (27) Velkov, T., Thompson, P. E., Nation, R. L., and Li, J. (2010) Structure–activity relationships of polymyxin antibiotics. *J. Med. Chem.* 53 (5), 1898–1916.
- (28) Azad, M. A., Finnin, B. A., Poudyal, A., Davis, K., Li, J., Hill, P. A., Nation, R. L., and Velkov, T. (2013) Polymyxin B induces apoptosis in kidney proximal tubular cells. *Antimicrob. Agents Chemother.* 57 (9), 4329–4335.
- (29) Azad, M. A., Akter, J., Rogers, K. L., Nation, R. L., Velkov, T., and Li, J. (2015) Major pathways of polymyxin-induced apoptosis in rat kidney proximal tubular cells. *Antimicrob. Agents Chemother.* 59 (4), 2136–2143.
- (30) Appelmelk, B. J., Su, D., Verweij-van Vught, A. M., Thijs, B. G., and MacLaren, D. M. (1992) Polymyxin B-horseradish peroxidase conjugates as tools in endotoxin research. *Anal. Biochem.* 207 (2), 311–316.
- (31) Velkov, T., Roberts, K. D., Nation, R. L., Wang, J., Thompson, P. E., and Li, J. (2014) Teaching ‘old’ polymyxins new tricks: new-generation lipopeptides targeting Gram-negative ‘superbugs’. *ACS Chem. Biol.* 16 (9), 1172–1177.
- (32) de Visser, P. C., Kriek, N. M., van Hooft, P. A., Van Schepdael, A., Filippov, D. V., van der Marel, G. A., Overkleef, H. S., van Boom, J. H., and Noort, D. (2003) Solid-phase synthesis of polymyxin B1 and analogues via a safety-catch approach. *J. Pept. Res.* 61 (6), 298–306.
- (33) O’Dowd, H., Kim, B., Margolis, P., Wang, W., Wu, C., Lopez, S. L., and Blais, J. (2007) Preparation of tetra-Boc-protected polymyxin B nonapeptide. *Tetrahedron Lett.* 48 (11), 2003–2005.
- (34) Okimura, K., Ohki, K., Sato, Y., Ohnishi, K., and Sakura, N. (2007) Semi-synthesis of polymyxin B (2–10) and colistin (2–10) analogs employing the trichloroethoxycarbonyl (Troc) group for side chain protection of alpha,gamma-diaminobutyric acid residues. *Chem. Pharm. Bull.* 55 (12), 1724–1730.
- (35) Okimura, K., Ohki, K., Sato, Y., Ohnishi, K., Uchida, Y., and Sakura, N. (2007) Chemical conversion of natural polymyxin B and colistin to their N-terminal derivatives. *Bull. Chem. Soc. Jpn.* 80 (3), 543–552.
- (36) Sakura, N., Itoh, T., Uchida, Y., Ohki, K., Okimura, K., Chiba, K., Sato, Y., and Sawanishi, H. (2004) The contribution of the N-terminal structure of polymyxin B peptides to antimicrobial and lipopolysaccharide binding activity. *Bull. Chem. Soc. Jpn.* 77 (10), 1915–1924.
- (37) Chihara, S., Yahata, M., Tobita, T., and Koyama, Y. (1974) Chemical synthesis and characterization of n-fattyacyl mono-aminoacyl derivatives of colistin nonapeptide. *Agric. Biol. Chem.* 38, 1767–1777.
- (38) Chihara, S., Yahata, M., Tobita, T., and Koyama, Y. (1974) Chemical synthesis, isolation and characterization of α -N-fattyacyl colistin nonapeptide with special reference to the correlation between antimicrobial activity and carbon number of fattyacyl moiety. *Agric. Biol. Chem.* 38, 521–529.
- (39) Tsubery, H., Ofek, I., Cohen, S., and Fridkin, M. (2001) N-terminal modifications of polymyxin B nonapeptide and their effect on antibacterial activity. *Peptides* 22 (10), 1675–1681.
- (40) Vaara, M. (1991) The outer membrane permeability-increasing action of linear analogues of polymyxin B nonapeptide. *Drugs Exp. Clin. Res.* 17 (9), 437–443.
- (41) Magee, T. V., Brown, M. F., Starr, J. T., Ackley, D. C., Abramite, J. A., Aubrecht, J., Butler, A., Crandon, J. L., Dib-Hajj, F., Flanagan, M. E., Granskog, K., Hardink, J. R., Huband, M. D., Irvine, R., Kuhn, M., Leach, K. L., Li, B., Lin, J., Luke, D. R., MacVane, S. H., Miller, A. A., McCurdy, S., McKim, J. M., Jr., Nicolau, D. P., Nguyen, T. T., Noe, M. C., O’Donnell, J. P., Seibel, S. B., Shen, Y., Stepan, A. F., Tomaras, A. P., Wilga, P. C., Zhang, L., Xu, J., and Chen, J. M. (2013) Discovery of Dap-3 polymyxin analogues for the treatment of multidrug-resistant Gram-negative nosocomial infections. *J. Med. Chem.* 56 (12), 5079–5093.
- (42) Deris, Z. Z., Swarbrick, J. D., Roberts, K. D., Azad, M. A., Akter, J., Horne, A. S., Nation, R. L., Rogers, K. L., Thompson, P. E., Velkov, T., and Li, J. (2014) Probing the penetration of antimicrobial polymyxin lipopeptides into Gram-negative bacteria. *Bioconjugate Chem.* 25 (4), 750–760.
- (43) Azad, M. A., Huang, J. X., Cooper, M. A., Roberts, K. D., Thompson, P. E., Nation, R. L., Li, J., and Velkov, T. (2012) Structure–activity relationships for the binding of polymyxins with human alpha-1-acid glycoprotein. *Biochem. Pharmacol.* 84 (3), 278–291.
- (44) Meredith, J. J., Dufour, A., and Bruch, M. D. (2009) Comparison of the structure and dynamics of the antibiotic peptide polymyxin B and the inactive nonapeptide in aqueous trifluoroethanol by NMR spectroscopy. *J. Phys. Chem. B* 113 (2), 544–551.
- (45) Pristovsek, P., and Kidric, J. (1999) Solution structure of polymyxins B and E and effect of binding to lipopolysaccharide: an NMR and molecular modeling study. *J. Med. Chem.* 42 (22), 4604–4613.
- (46) Pristovsek, P., and Kidric, J. (2004) The search for molecular determinants of LPS inhibition by proteins and peptides. *Curr. Top. Med. Chem.* 4 (11), 1185–1201.
- (47) Tsubery, H., Ofek, I., Cohen, S., and Fridkin, M. (2002) Structure–activity relationship study of polymyxin B nonapeptide. *Adv. Exp. Med. Biol.* 479, 219–222.
- (48) Vaara, M., Siikanen, O., Apajalahti, J., Fox, J., Frimodt-Moller, N., He, H., Poudyal, A., Li, J., Nation, R. L., and Vaara, T. (2010) A novel polymyxin derivative that lacks the fatty acid tail and carries only three positive charges has strong synergism with agents excluded by the intact outer membrane. *Antimicrob. Agents Chemother.* 54 (8), 3341–3346.
- (49) Vaara, M., and Vaara, T. (2013) The novel polymyxin derivative NAB739 is remarkably less cytotoxic than polymyxin B and colistin to human kidney proximal tubular cells. *Int. J. Antimicrob. Agents* 41 (3), 292–293.
- (50) Vaara, M., Fox, J., Loidl, G., Siikanen, O., Apajalahti, J., Hansen, F., Frimodt-Moller, N., Nagai, J., Takano, M., and Vaara, T. (2008) Novel polymyxin derivatives carrying only three positive charges are

effective antibacterial agents. *Antimicrob. Agents Chemother.* 52 (9), 3229–3236.

(51) Velkov, T., Thompson, P. E., Nation, R. L., and Li, J. (2010) Structure–activity relationships of polymyxin antibiotics. *J. Med. Chem.* 53 (5), 1898–1916.

(52) Voitenko, V. G., Bayramashvili, D. I., Zebrev, A. I., and Zinchenko, A. A. (1990) Relationship between structure and histamine releasing action of polymyxin B and its analogues. *Agents Actions* 30 (1–2), 153–156.

(53) Pristovsek, P., and Kidric, J. (2004) The search for molecular determinants of LPS inhibition by proteins and peptides. *Curr. Top. Med. Chem.* 4 (11), 1185–1201.

(54) Hancock, R. E. (1997) The bacterial outer membrane as a drug barrier. *Trends Microbiol.* 5 (1), 37–42.

(55) Hancock, R. E. (1997) Peptide antibiotics. *Lancet* 349 (9049), 418–422.

(56) Hancock, R. E., and Lehrer, R. (1998) Cationic peptides: a new source of antibiotics. *Trends Biotechnol.* 16 (2), 82–88.

(57) Li, J., Milne, R. W., Nation, R. L., Turnidge, J. D., and Coulthard, K. (2003) Stability of colistin and colistin methanesulfonate in aqueous media and plasma as determined by high-performance liquid chromatography. *Antimicrob. Agents Chemother.* 47 (4), 1364–1370.

(58) Roberts, K. D., Azad, M. A. K., Wang, J., Horne, A. S., Thompson, P. E., Nation, R. L., Velkov, T., and Li, J. (2015) Antimicrobial activity and toxicity of the major lipopeptide components of polymyxin B and colistin: last-line antibiotics against multidrug-resistant Gram-negative bacteria. *ACS Infect. Dis.* 1 (11), 568–575.

(59) Wayne, P. A. (2013) *Performance Standards for Antimicrobial Susceptibility Testing*, 23rd Informational Supplement M100-S23, Clinical and Laboratory Standards Institute.